 © ASM International

Effect of Rare Earth and Calcium Treatments on the Mechanical, Physical, and Electrochemical Properties of a 16Mn Steel

Longquan Shi, Jizhi Chen, and Derek O. Northwood

Two treatment methods, namely Ca-Si injection into the ladle and rare earth (RE) additions to the mold, were investigated for their effectiveness in controlling the microstructure, particularly sulfide inclusions, and hence the properties of a 16Mn plain-carbon steel. A combined Ca + RE treatment increased the critical crack opening displacement in the transverse direction of sheet material to that in the rolling direction. The combined treatment also improved the resistance to stress-corrosion cracking (SCC) in a boiling 20 wt.% NH_4NO_3 solution. Too large a RE addition, ultimately lowers SCC resistance. The RE additions retarded austenite grain growth, whereas the Ca-only addition accelerated grain growth. The changes in fracture behavior, SCC resistance, and austenite grain growth behavior are explained in terms of the segregation of the RE to the grain boundaries and the subsequent changes in the electrochemical and mechanical properties of the grain boundaries relative to the grain interiors. A combined treatment of injecting 3.4 kg Ca-Si per ton of steel into the molten steel and adding 0.03 wt.% RE to the mold yielded optimum properties.

1 Introduction

In a previous paper,[1] two treatment methods, namely Ca-Si injection into the ladle and rare earth (RE) additions to the mold, were investigated for their effectiveness in controlling the sulfide inclusions in a 16Mn steel. It was shown that Ca desulfurization did not completely remove all of the MnS inclusions and that the RE inclusion shape modification treatment increased the amount of inclusions compared to using only a Ca treatment. A combined RE plus Ca treatment was shown to give the best control of inclusion shape, amount, and distribution. The combination treatment also provided a relatively homogeneous distribution of Mn in the banded (ferrite + pearlite) structure of hot rolled sheet.

This previous work[1] was entirely microstructural in nature, and it was of interest to determine whether these microstructural improvements translated into improvements in the properties of the steel. In the present study, certain mechanical, physical, and electrochemical properties of the steel were determined for hot-rolled sheet. In agreement with the microstructural studies, the combined treatment (Ca desulfurization followed by RE inclusion shape control) yielded optimum property improvements in the steel.

2 Experimental Details

2.1 *Materials*

The 16Mn steel used in this study is a plain-carbon steel that is similar to AISI 1020 steel with respect to its chemical composition.[2] The steel was refined in a 300-ton open hearth furnace. A two-ladle system was used—Ladle A had no Ca-Si injected and Ladle B was injected with 3.4 kg of Ca-Si per ton of steel. The steel from these ladles was poured into molds with different RE contents (see Table 1 for full details of treatments of the six ingots). The flat ingots, which each weighed 12.5 tons, were hot rolled into sheet 6 mm thick and 1100 mm wide. The typical chemical composition at the midpoint of the ingots was 0.19% C, 1.4% Mn, 0.41% Si, and 0.023% P (all compositions in wt.%). The specimens for the present tests were taken from the middle, with respect to the width, of the sheet at a location corresponding to the middle (with respect to the top-bottom) of the ingot. The actual chemical compositions for S, Ca, and RE of the rolled sheet from the six ingots are given in Table 2.

2.2 *Critical Crack Opening Displacement Measurements*

Critical crack opening displacement (COD), δ_c, measurements were made on the three-point bend specimens with the following dimensions: length (L) of 50 mm, width (W) of 10 mm, and thickness (B) of 5 mm. The bend gauge length (S) was 40 mm. The specimens had a 3-mm machined notch and a 2-mm preset fatigue crack (the fatigue crack was produced on a 400-kg high-frequency fatigue test machine using loads of $P_f$max = 140

Table 1 Treatment Methods for Steels

Steel ingot No.	Ladle No.	Ca-Si treatment in ladle, kg of Ca-Si/ton of steel	RE addition to mold, wt.%
6	A	...	...
5	A	...	0.1
4	B	3.4	...
3	B	3.4	0.03
2	B	3.4	0.06
1	B	3.4	0.1

Longquan Shi, Engineering Materials Group, University of Windsor, Windsor, Ontario, Canada; presently on leave from Materials Division, Beijing General Research Institute of Mining and Metallurgy, Beijing, The People's Republic of China; **Jizhi Chen,** Institute of Metal Research, Academia Sinica, Shenyang, P.R. China; and **Derek O. Northwood,** Engineering Materials Group, University of Windsor, Windsor, Ontario, Canada.

Table 2 Chemical Composition Analysis of Rolled Sheet

Ingot No.	Composition, wt.% S	RE	Ca
6	0.021	0	0
5	0.021	0.035	0
4	0.0082	0	0.0065
3	0.0076	0.014	0.0048
2	0.0047	0.036	0.0028
1	0.0061	0.066	0.0042

kg and $P_f$min = 20 kg). The test procedure and the data processing followed the National Standard of the People's Republic of China (PRC GB2358-80). The material constants used for the calculation were as follows: Young's modulus (E) = 2.1×10^4 kg/mm^2 (206 GPa), yield strength (σ_y) = 43.4 kg/mm^2 (425 MPa), Poisson's ratio (ν) = 0.30 and plastic zone correction factor (rp) = 0.45. To avoid any (crack) size change due to plastic deformation, following the three-point bend tests the specimens were then broken by a second fatigue cracking, prior to the bending crack extension length (Δa) measurement being made. A bluing treatment of 300 °C for 1 hr was used on all of the bend specimens prior to second fatigue cracking to delineate the crack due to bending from the preset fatigue crack and the second fatigue crack.

2.3 *Stress-Corrosion Cracking Tests*

The tensile specimens for the stress-corrosion cracking (SCC) tests were taken from the L (rolling) direction in the sheet. They had a diameter of 5 mm and a gauge length of 10 mm. The corrosive medium was a boiling 20 wt.% NH_4NO_3 solution. The testing temperature was maintained at 104 °C. All tests were conducted under a constant load. The initial tensile stress, σ, and the SCC fracture life, t_f, were recorded for each alloy over a range of tensile stresses.

2.4 *Austenite Grain Growth Experiments*

The specimens for the austenite grain growth experiment were 5 mm by 10 mm by 10 mm cubes. They were sealed in quartz tubes, which were first pumped to a high vacuum (10^{-5} torr, 1.3 mPa) and were back-filled with high-purity Ar gas to a pressure of 300 torr (40 kPa). Each quartz tube had one specimen from each of the six different ingots. Two sets of austenitic grain growth experiments were carried out. In the first set, each set of specimens was heated for 10 min at four different temperatures (930, 980, 1020, and 1080 °C). In the second set, each set of specimens was heated at the same temperature (980 °C) for different periods of time up to 600 min. The heated samples were water quenched to retain the austenitic grain size present at the high temperature. The grain boundaries were revealed by etching with a picric acid solution at 80 °C for about 4 min. The average austenitic grain size was measured using optical microscopy and a line intercept method. Some 50 different locations were counted on each specimen.

2.5 *Microhardness and Electrical Potential Measurements: Differences Between Grain Boundaries and Grain Interiors*

Microhardness measurements were made of both the αFe grain interiors and grain boundary regions for sheet from all six ingots. The measurements were made using an indenting load of 5 g and a Neopton 2-type microhardness system. The results are presented as a microhardness difference, ΔH_m, between the grain interior and the grain boundary.

For the electrical potential tests, two sets of specimens were prepared. One set of specimens had a polished surface. The other set contained specimens with an intergranular fracture surface, which was obtained by a Charpy impact test of notched specimens at –32 °C. The samples with an intergranular fracture surface were kept in acetone to avoid contamination of the fracture surface. The solution used for the electrical potential tests was a 0.038 wt.% picric acid solution. The test temperature was 22 °C. The "non-test" surface was wrapped in PTFE tape. Measurements were made on each specimen for a period up to about 3 hr, at which time a steady-state electrical potential was obtained. The potential measured for the fracture surface was higher than that for the polished surface. The potential difference, ΔE, measured between the fracture surface and the polished surface, is taken as being equivalent to the potential difference between the grain boundaries and the grain interiors.

2.6 *Secondary Ion Mass Spectrometry Depth Analysis*

Secondary ion mass spectrometry (SIMS) was only carried out on one specimen, namely the sheet from Ingot 1, and was designed to determine the segregation of the rare earths in the grain boundaries of the steel. An intergranular fracture surface was first obtained using the same method as that described in Section 2.5 for the electrical potential measurements. The specimen was examined in a model LT-1A ion probe mass spectrometer. The relative intensity of $^{140}Ce^+$ was taken as being representative of the rare earth concentration. The data are obtained in the form of an intensity of $^{140}Ce^+$ versus time plot. The time is proportional to the depth from the grain boundary (the surface is being ion beam milled away). The SIMS analysis experimental parameters were as follows: the primary ion was O_2^+, the first ion beam diameter was 50 μm, the voltage was 16 kV, and the beam current was 2×10^{-6} A. The secondary ion accelerating voltage was 1500 V and the vacuum was 10^{-6} torr.

3 Experimental Results

3.1 *Critical Crack Opening Displacement at Room Temperature*

A number of researchers have used the Charpy impact test to determine the effects of RE additions on the fracture toughness and the ductile-brittle transition temperature of steels.[3,4] In the current study, critical crack opening displacement, δ_c was measured, because δ_c is an "absolute" property of the crack propagation, unlike the impact toughness (such as obtained from the Charpy test) which is influenced by a crack nucleation factor.[5-7] The δ_c criterion is suitable for steels that have high ductility,[5-7] including steels used in pressure vessels and piping.

Table 3 Results of Crack Opening Displacement Tests

Ingot No.	δ_c, mm	
	L direction	*T* direction
6	0.15	0.086
5	0.15	0.15
4	0.15	0.10
3	0.15	0.15
2	0.15	0.15
1	0.15	0.15

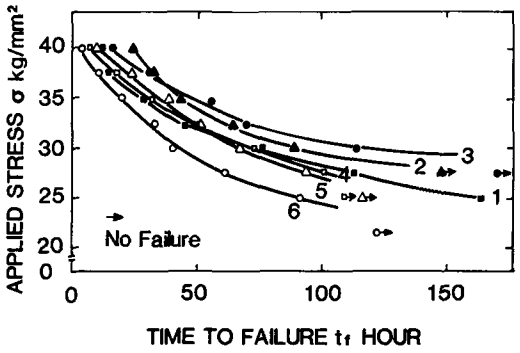

Fig. 1 Time to failure, (t_f), versus initial applied stress for SCC tests in boiling NH_4NO_3 solution.

The critical COD for high toughness, relatively low strength materials is an excellent comparative toughness parameter.[5]

The results for δ_c, the critical crack opening displacement, for the six different ingots are given in Table 3. For the *L* (rolling) direction, all δ_c values are approximately 0.15 mm and did not significantly change with the Ca and/or RE treatment. In the *T* (transverse or width) direction, sheet from the untreated ingot (No. 6) had the lowest δ_c value (0.086 mm). Sheet from Ingot 4, which was only treated by Ca-Si, had a δ_c value (0.10 mm) that was lower than in the *L* direction. Sheet from all the ingots with the combined Ca-Si and RE treatment had a δ_c value equal to that in the *L* direction, *i.e.*, 0.15 mm.

3.2 *Stress-Corrosion Cracking Tests*

The aim in these tests was to investigate the effects of RE additions on the stress-corrosion cracking behavior, especially for intergranular failure. The samples were all taken in the *L* direction of the sheet so as to eliminate any effects due to the direction of the inclusions and the banded structure. A boiling 20 wt.% NH_4NO_3 solution was selected so as to ensure crack propagation along the grain boundaries.[8] The results are shown in Fig. 1 as a plot of applied tensile stress, σ, versus the time to fracture, t_f. The best SCC resistance is exhibited by specimens for the sheet made from Ingot 3, *i.e.*, Ca + RE treatment. The addition of only 0.1% RE increases the time to fracture (compare Ingot 6, untreated, with Ingot 5, RE treatment only), but a combined treatment, *i.e.*, adding the RE after injecting Ca-Si, further increases the time to failure. The intergranular nature of the SCC failure was confirmed by optical metallography of polished specimens (Fig. 2a) and SEM observations of the fracture surface (Fig. 2b).

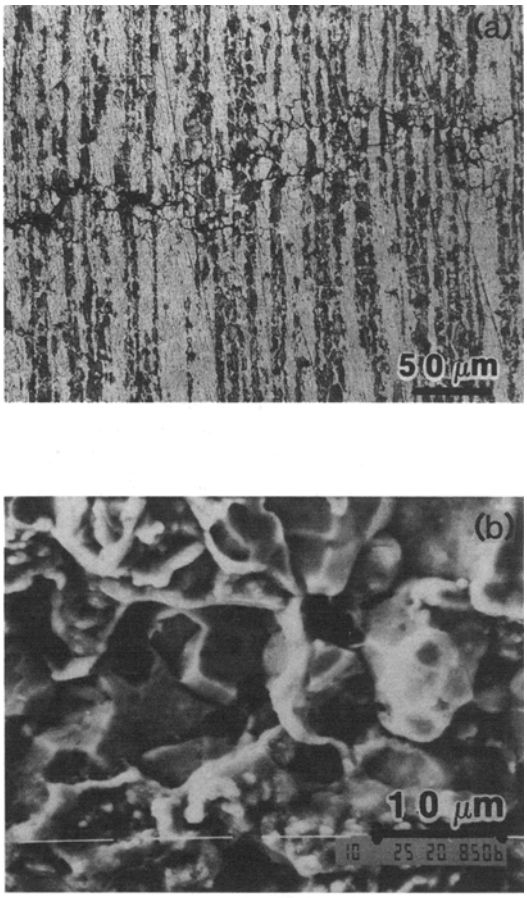

Fig. 2 (a) Optical micrograph showing intergranular crack propagation due to SCC of a 16Mn steel in a boiling NH_4NO_3 solution. (b) SEM micrograph showing morphology of SCC fracture surface of 16Mn steel in a boiling NH_4NO_3 solution.

3.3 *Austenite Grain Growth*

Figure 3 summarizes the results of austenite grain growth experiments. Figure 3(a), a grain size-temperature plot, indicates that the sheet from Ingot 6 (untreated) is the best for resisting high-temperature (1080 °C) grain growth and that the sheet from Ingot 4 (Ca-only treatment) is the poorest. However, the results given in Fig. 3(a) are for a short time (10 min), and trends can change with longer heating times. For instance, the results in Fig. 3(b), a grain size versus heating time at 980 °C plot, show that the grain size of the sheet from Ingot 6 (untreated) is larger than that for the sheet from Ingot 5 (RE only) after heating for times longer than about 260 min.

Figure 3(a) clearly shows that adding Ca (Ingot 4) decreases the temperature at which there is significant austenite grain growth, but that this can be offset by the addition of RE (compare sheet from Ingot 4 with sheet from Ingots 3, 2, or 1). The combined treatment, *i.e.*, injecting Ca-Si into the ladle and adding RE in the mold, is particularly effective for small RE additions at low heating temperatures, *e.g.*, ≤1000 °C—compare results for Ingot 4 (Ca only) with Ingot 3 (Ca + 0.03%

RE)—whereas at higher temperatures the larger the RE addition the more effectively it prevents austenite grain growth.

The isothermal kinetics at 980 °C (Fig. 3b), show that adding RE only can slow the long-term austenite grain growth (compare Ingots 5 and 6). The Ca-only treatment, however, accelerates the grain growth (compare Ingot 4 with Ingot 6). The data for the combined Ca + RE treatments (Ingots 3, 2, and 1) show that an increase in RE addition slows the isothermal austenite grain growth, *i.e.*, the data demonstrate the same trends as shown by the isochronal data.

3.4 *Microhardness and Electrical Potential Measurements at Grain Boundaries and Grain Interiors*

As noted in Section 2.5, the microhardness was measured in both the αFe grain interiors and at the grain boundaries, and a hardness difference, ΔH_m was determined. Figure 4, which summarizes the results of microhardness testing, shows that ΔH_m decreases with increasing RE content. A combined treatment, *i.e.*, injecting Ca-Si and adding RE, decreases ΔH_m more significantly than adding RE only.

As described in Section 2.5, specimens for the electrical potential tests either had a polished surface (taken as potential of grain interiors) or an intergranular fracture surface (taken as potential of grain boundaries). Figure 5, which summarizes the results for the electrical potential difference (ΔE) between the grain boundaries and grain interiors, clearly shows that adding RE or injecting Ca-Si alone decreases ΔE. The combined treatment, however, decreases ΔE more significantly. The greater the RE addition to the steel, the smaller ΔE.

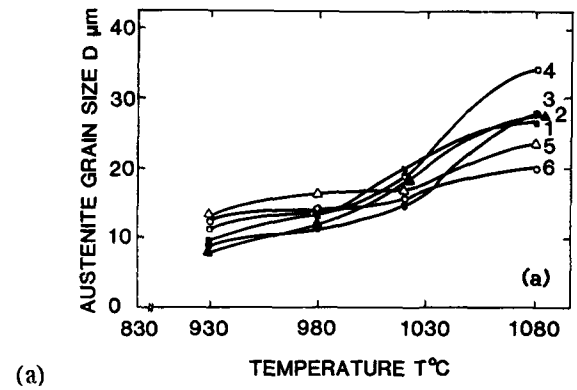

(a)

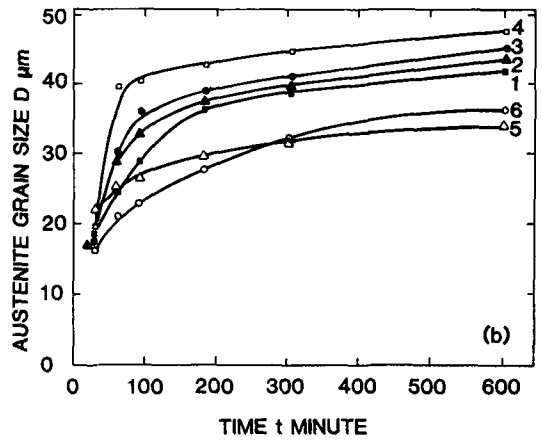

(b)

Fig. 3 Temperature and time dependence of austenite grain growth. (a) Austenite grain size versus temperature for 10-min heat treatment. (b) Austenite grain size versus time for heating at 980 °C.

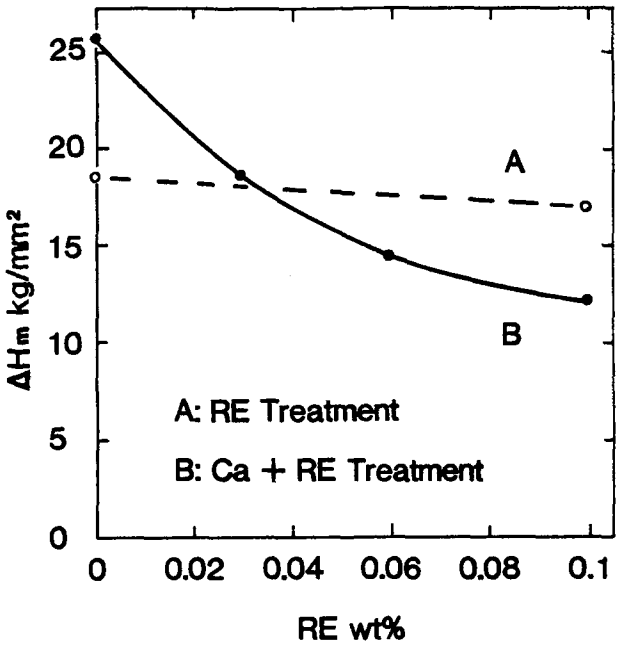

Fig. 4 Relationship between microhardness difference, ΔH_m, recorded between the grain boundaries and the grain interiors, and the amount of RE addition.

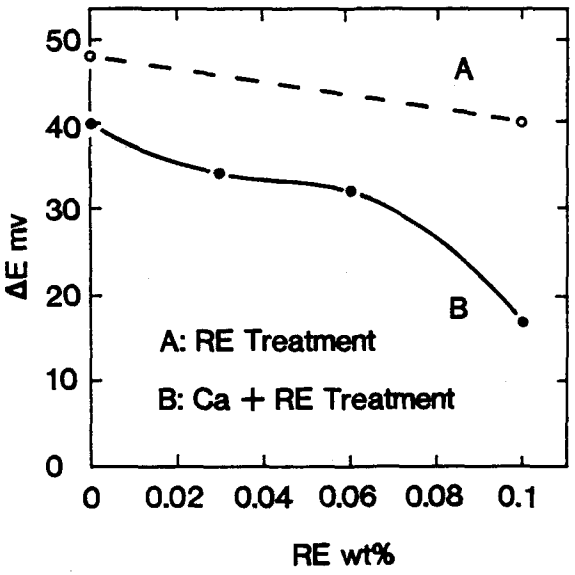

Fig. 5 Relationship between electrical potential difference, ΔE, recorded between the grain boundaries and the grain interiors, and the amount of RE addition.

3.5 *Ion Probe Analysis*

The depth distribution of $^{140}Ce^{+}$ from the grain boundary fracture surface in the sheet from Ingot 1 was determined and is shown in Fig. 6. The RE element segregates to the grain boundaries in the RE treated steel. The RE concentration decreases away from the grain boundaries (increasing time) and approaches a "constant" value in the grain interior.

The equilibrium segregation of the RE alloying elements to grain boundaries decreases the energy of the grain boundaries.[9] This is demonstrated quite clearly in the electrochemical measurements given in Section 3.4 for the 16Mn steel.

4 Discussion

4.1 *Effect of Inclusions on the Nucleation and Propagation of Cracks*

Elongated inclusions that are present in steel can give rise to a stress concentration.[10] A crack will be created by the stress concentrations at the inclusion and the pile-up of dislocations against the inclusion (see Fig. 7). In the *L* direction, the MnS inclusions have no effect on the crack propagation, because the inclusion is perpendicular to the extension direction of the crack. It is a different case in the *T* (transverse) direction, because the crack induced by both the inclusion stress concentration $q\sigma\psi$, and the pile-up dislocation stress concentration, $q_1\tau_\theta$, lies in the same direction as the crack extension. The results for the critical crack opening displacement, δ_c, measurements in the *T* direction show that the sheet from Ingots 6 and 4, which have some elongated inclusions (see Ref 1 for details), have a smaller δ_c than that of the sheet from Ingot 5, 3, 2, and 1, which were treated with RE additions. The combined treatment of adding RE to the mold and injecting Ca-Si into the ladle eliminates the anisotropy in the δ_c values.

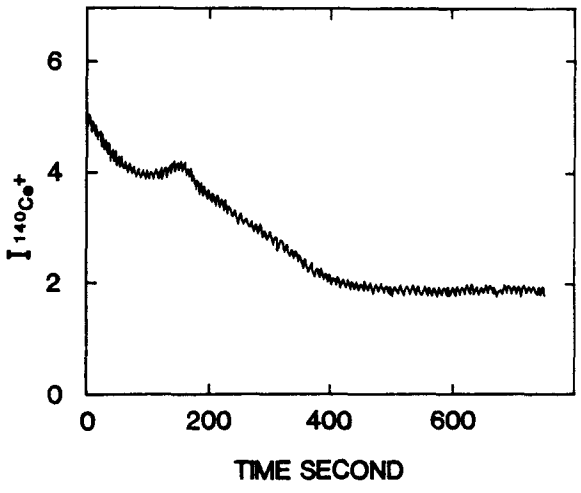

Fig. 6 SIMS results showing the RE content (Ce) versus depth from fracture surface, *i.e.*, grain boundary, for sheet made from Ingot 1.

4.2 *Grain Boundary Effects of RE Additions*

The effects of small RE additions to steel have recently attracted some attention. These effects can, in general, be classified into two groups.[11] The first group comprises effects that are induced by some interaction between the RE element and interstitial atoms in the steel, *e.g.*, prevention of precipitation, coalescence, and growth of carbides in martensite during annealing, etc. The second group consists of effects in which there is a property change due to a concentration of RE elements at the grain boundaries, *e.g.*, RE elements can reduce or prevent fracture along grain boundaries of steels containing phosphorus and reduce temper brittleness of steels. The two types of effects usually coexist.

It should be noted that the RE elements can be segregated at the grain boundaries in one or both of two forms, namely as inclusions and/or in solid solution. Thus, the RE addition may have different effects on properties of steel depending on its form. Solid solution RE elements segregated at the grain boundary are beneficial to properties, but an increasing number of RE inclusions will cause property degradation. In this situation, a small amount of RE addition will improve the properties, but when the RE addition exceeds a certain limit properties deteriorate. It is also possible for both the solid solution RE elements and the dispersed RE inclusions at the grain boundaries to be advantageous to some properties. In this situation, the higher the RE addition, the better the property improvement. In the current studies, the results of the tests on stress-corrosion cracking in the boiling NH_4NO_3 solution and the austenite grain growth studies are good examples of these two different situations.

4.2.1 *Effect of RE Additions on Stress-Corrosion Cracking*

The addition of the RE changes the electrochemical properties of the grain boundaries. By decreasing the grain boundary energy, that is the chemical activity of atoms at grain boundaries,

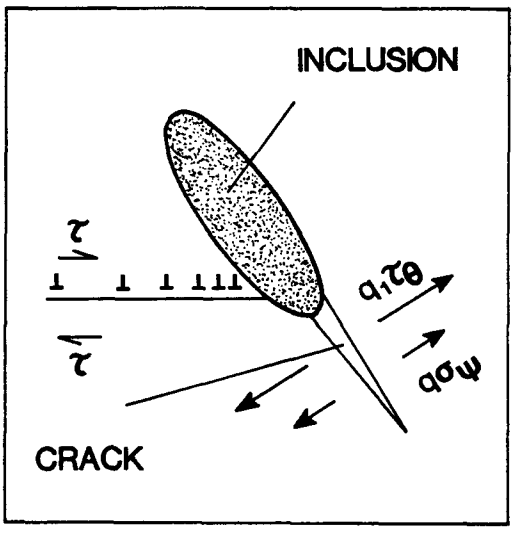

Fig. 7 Schematic diagram showing how stress concentrations at inclusion, $q\sigma\psi$, and at pile-up of dislocations, $q_1\tau_\theta$ can induce crack.

RE additions decrease the chemical heterogeneity between the grain boundaries and the grain interiors. This, in turn, decreases the potential of the microelectronic cell, *i.e.*, local galvanic cell at grain boundaries, which controls a rate of dissolution and the rate of crack extension by selective attack at the grain boundaries. This type of argument can be used to explain the effects of RE additions on the stress-corrosion cracking of carbon steels in the solutions containing NO_3^- ion, where corrosion (dissolution processes) dominates.[12] The corrosion of the grain boundaries is slowed by the RE treatment and the propagation of a crack along the pre-existing active path, the grain boundary, becomes slower.[12,13] This has been confirmed by the measurement of electrical potential difference between microzones of the grain boundary and the inner grain.[12,13] Such an electrical potential difference will produce quite a large local dissolution current at grain boundaries, which accelerates the crack dissolution along the grain boundaries during stress-corrosion cracking.

In the present study, the steady-state electrical potential difference between a fractured surface and a polished surface was measured to probe the chemical homogeneity of the grain boundaries and the grain interiors of the steel. The results show that, with increasing RE addition, the potential difference, ΔE, decreases. That is to say that the RE addition increases the electrochemical homogeneity. Secondly, the RE concentrating in grain boundary gives rise to a strengthening of the grain boundary. This is clearly shown in the microhardness tests. Both these factors contribute to the improved resistance of the 16Mn steel to SCC along the grain boundaries. However, when the RE addition exceeds a certain limit, there will be a large number of inclusions in the steel, which is in itself disadvantageous to SCC resistance. The ingot with the combined treatment, *i.e.*, injecting Ca-Si into the ladle and adding 0.003 wt.% RE to the mold, has the highest resistance to SCC.

4.2.2 *Effect of RE Additions on Austenite Grain Growth*

The experimental results show that, whereas the RE additions increased the temperature or time required for significant austenite grain growth, the injection of Ca-Si accelerated the grain growth process. The effects of different RE additions following Ca-Si treatment were such that a small amount of RE addition prevented austenite grain growth at relative lower temperatures, but that a larger RE addition is required to reduce grain growth at higher temperatures. The reason for this observed behavior is the fact that RE addition decreases the grain boundary energy of austenite (as seen from electrical potential measurements).

The austenite grain growth results show quite clearly the different effects of the two alloy elements RE and Ca. This can be understood better by looking at the analogy between grain growth and precipitate coarsening. According to the Lifshiz-Sylozov-Wagner (LSW) theory,[14-16] particle coarsening (Ostwald-Reifung ripening[17]) kinetics in a solid solution follows the relation:

$$\bar{r}_t^n - \bar{r}_o^n = K \cdot t \qquad [1]$$

where $\bar{r}_t$ and $\bar{r}_o$ are the average particle sizes at time t and at the onset of coarsening, respectively. For a diffusion-controlled growth mechanism, the exponential n equals 3 and the rate constant K in Eq 1 is given by:

$$K = \left[\frac{8\gamma DCe\, V_m^2}{9RT}\right] \qquad [2]$$

where γ is the interfacial free energy, D is the solute diffusivity, Ce is the equilibrium solute concentration, V_m is the molar volume of the precipitate, and R is the gas constant and T is temperature in degrees kelvin. In the grain growth case, γ becomes grain boundary energy. Suppose the parameters in the rate constant K equation (Eq 2) are the same for both RE and Ca-Si treatments, except for γ, D, and Ce. The different alloying elements in the steel may change both γ and D and have different values for Ce. Both the RE and Ca treatments decrease γ by their equilibrium segregation to the grain boundaries. However, the Ca treatment accelerated the austenite grain growth. This is probably due to an increase in the diffusivity, D, of the iron atoms, *i.e.*, Ca increases the γD factor in Eq 2. The RE, on the other hand, has a very small solubility, Ce, in steel (virtually equal to zero[18]) and a very small D value because of its large atomic size with respect to the iron atom. Thus, the RE treatment will give rise to a very small K value for austenite grain growth compared to that for Ca treatment.

Also, the combined treatment, Ca + RE, produces a fine dispersion of small, but stable, RE sulfide (RES) and oxysulfide particles. These particles can pin the austenite grain boundaries at high temperatures.[18] Once again, the RE treatment is superior to the Ca treatment with respect to its effectiveness in pinning the grain boundaries. For example, the RES has larger (more negative) free energy of formation, ΔG, than that of CaS over the temperature range 0 to 3000 °C,[18,19] *i.e.*, the RES particles are more stable than the CaS particles at higher temperatures.

5 Conclusions

Studies on a 16Mn steel (similar to AISI 1020 steel) have shown that a low-sulfur steel can be produced by injecting Ca-Si into the ladle. A RE addition to the mold further improves the properties of the steel. In particular, the addition of a RE to the mold following Ca-Si injection into the ladle:

- Increases the critical crack opening displacement δ_c in the T direction of the sheet to that of the L direction in the sheet and eliminates anisotropy.
- Improves the resistance of the steel to SCC in a boiling 20 wt.% NH_4NO_3 solution. However, too large a RE addition will ultimately lower SCC resistance.
- Decreases the steady-state electrical potential difference between the fracture surface and the polished surface of the steel (*i.e.*, between the grain boundaries and the grain interiors).
- Decreases the microhardness difference between the grain interiors and grain boundaries.
- Increases the temperature for austenite grain growth, *i.e.*, retards austenite grain growth.

Acknowledgment

The work described formed part of the M.Sc. thesis research of one of the authors (L. Shi). The authors are grateful for the facilities provided by the Stress Corrosion Laboratory, Institute of Corrosion Research, Academia Sinica, Shenyang, P.R. China. The steel was provided by the Anshan Iron and Steel Corporation, Anshan, P.R. China. Continued financial support to L. Shi is being provided by the Natural Sciences and Engineering Research Council of Canada through an Operating Grant (A4391) awarded to Prof. D.O. Northwood.

References

1. L. Shi, J. Chen, and D.O. Northwood, Inclusion Control in a 16 Mn Steel Using a Combined Rare Earth and Calcium Treatment, *J. Mater. Eng.*, 13, 273-279 (1991).
2. W.F. Smith, *Structure and Properties of Engineering Alloys*, McGraw-Hill, New York, 87 (1981).
3. L. Luyckx, J.R. Bell, A. McLean, and M. Korchynsky, Sulfide Shape Control in High Strength Low Alloy Steels, *Metall. Trans.*, *1*, 3341-3350 (1970).
4. G.E. Dieter, *Mechanical Metallurgy*, 2nd ed., McGraw-Hill, New York, 274 and 502 (1976).
5. D. Broek, *Elementary Engineering Fracture Mechanics*, 4th ed., Martinus Nijhoff Publishers, Dordrecht, The Netherlands, 24 (1986).
6. A.A. Wells, Unstable Crack Propagation in Metals: Cleavage and Fast Fracture, *Proc. Crack Propagation Symposium*, College of Aeronautics and the Royal Aeronautical Society, Cranfield, England, 210-230 (1961).
7. A.A. Wells, Welding of Vessels for Low-Temperature Service in Britain, *British Welding Res. Ass. Rept.*, Cambridge, England, M13/63 (1963).
8. M.J. Humphries and R.N. Parkins, The Influence of Oxide Films on Stress-Corrosion Cracking of Carbon Steels, *Proc. Conf. Fundamental Aspects of Stress-Corrosion Cracking*, National Association of Corrosion Engineers, Houston, Texas 384-395 (1969).
9. D. McLean, *Grain Boundaries in Metals*, The Clarendon Press, Oxford, 116 (1957).
10. R.H. Edwards, Stress Concentrations Around Spheroidal Inclusions and Cavities, *J. Appl. Mech. Trans. ASME*, *73*, 19-30 (1951).
11. J. Chen, The Distribution of Rare Earth in Steel Ingot and Its Effects on the Mechanical Properties of the Steel Sheet, in *Collected Works for Commemorating Li Xun*, Science Press, Beijing 210-220 (1986) in Chinese.
12. R.N. Parkins, Stress Corrosion Spectrum, *Brit. Corr. J.*, *7*, 15-28 (1972).
13. R.N. Parkins, Stress Corrosion Cracking, *Corrosion and Protection*, (2), 43-51 (1982) in Chinese.
14. I.M. Lifshitz and V.V. Sylozov, The Kinetics of Precipitation From Supersaturation Solid Solutions, *J. Phys. Chem. Solids*, *19*, 35-50 (1961).
15. C. Wagner, Theorie der Alterung von Niederschlägen durch Umlösen (Ostwald-Reifung), *Z. Electrochem.*, *65*, 581-591 (1961).
16. J.W. Martin and R.D. Doherty, *Stability of Microstructure in Metallic Systems*, Cambridge University Press, Cambridge, 186 (1976).
17. W. Ostwald, Über die vermeinttiche Isomerie des roten und gelben Quecksilberoxyds und die Oberflachenspannung fester Körper, *Z. Phys. Chem.*, *34*, 495-503 (1900).
18. L.A. Luyckx, The Rare Earth Metals in Steel, in *Industrial Applications of Rare Earth Elements*, ACS Symposium Series 164, K.A. Gschneidner, Jr., Ed., American Chemical Society, Washington, DC, 34-78 (1981).
19. A.H. Cottrell, *An Introduction to Metallurgy*, 2nd ed., Edward Arnold Publishers Ltd., London, 83 (1975).